Speed limitations of Geiger-Müller counters

Speed Limitations of Geiger-Müller Counters

by **Hendrik den Hartog**.

Laboratory of Physics University of Amsterdam.

Summary. This paper summarizes the three main speed limitations imposed on the use of GEIGER-MÜLLER counters, viz. the electron transit time, the development of the discharge and the finite rise time of the pulse associated with it, and finally the deadtime. This deadtime is analysed more fully for low and high counting rates. Finally a technique is described for eliminating most of the complications connected with very high counting rates.

Migration of the Secondary Electrons.

GEIGER-MÜLLER counters consist of a small active and a large passive region, in the latter of which the ionization by the radiation under observation takes place.

A considerable time is required for the electrons liberated to migrate through the comparatively low field in the neighbourhood of the wall to the active region of the wire, where multiplication is initiated.

In contrast to newly developed secondary-emission devices, GEIGER-MÜLLER counters show an initial time lag caused by this effect. Measurements by SHERWIN[1]) and by MULLER, VAN ROODEN, VERSTER, and the author[2])[3]) have yielded a fairly complete, although not yet entirely consistent picture. In a typical counter of 30 mm cathode diameter and filled with 90 mm of argon and 10 mm of ethyl alcohol the maximum time lag is 0.35 microseconds. This time lag is roughly proportional to the alcohol pressure and to the square of the diameter but for the very smallest pressures and diameters, when the mobility might no longer be constant, and the additional time necessary for the first avalanches to develop to a detectable extent becomes relatively appreciable.

In Fig. 1, data are collected of electron transit times in the mixture just mentioned. Sherwin quotes a transit time of 0.1 microsecond for a radius travelled of 1 cm, in a filling of 92 mm Hg of argon and 8 mm of amyl-acetate. The measurements of Sherwin cover the high field-strength region of the counter, and do not seem to con-

form to a constant mobility. SHERWIN's findings can be described by the formula

$$v = 4.5 \left(\frac{F}{p}\right)^{\frac{1}{2}} \text{cm}/ \, \mu \, \text{sec.,}$$

where F is the field-strength in volt per cm, and p the total pressure in mm of Hg.

Data on the mobility k derived from the radii r travelled in times t by means of the formula $k = r^2/4tCV$ as published by the Dutch authors are shown in Fig. 2. Here C is the capacitance $1/2 \ln(r_c/r_a)$ per unit length of counter, and V is the voltage across it.
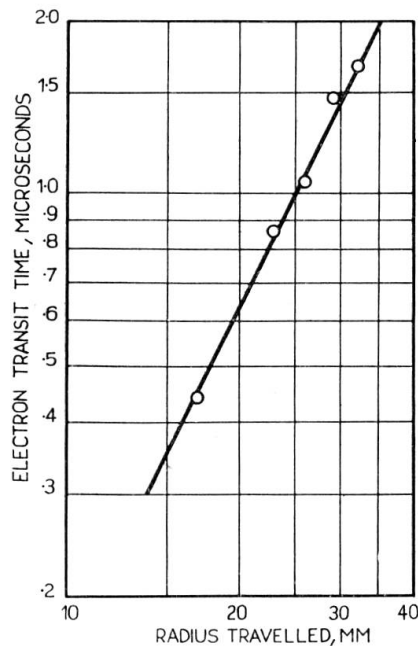
Fig. 1.

Electron transit times observed in a counter filling of 90 mm Hg of argon and 10 mm Hg of alcohol vapour. (Wire diameter 0.1 mm, cathode diameter 68 mm, operating voltage 1300 volts.)

From the experimental work of SHERWIN[1] and the theoretical investigations of WILKINSON[10] it appears that a second delay must be taken into account during which the avalanche activity develops to a detectable level. In consequence of the exponential nature of the development of the discharge, this delay cannot appreciably be reduced by increasing the amplification. In one specific instance, WILKINSON calculates an extra delay of 0.015 microseconds at 100 volts overvoltage, and of 0.06 at 30 volts overvoltage, but it must be remembered that this second delay depends critically on the photon free path, varying approximately as the square of this

quantity (counter data: cathode diameter 20 mm, wire diameter
0.2 mm; 65 mm Hg of argon and 5 mm of alcohol vapour).

Much shorter time lags can be obtained by using parallel-plate
counters, but most investigators have found it necessary to use
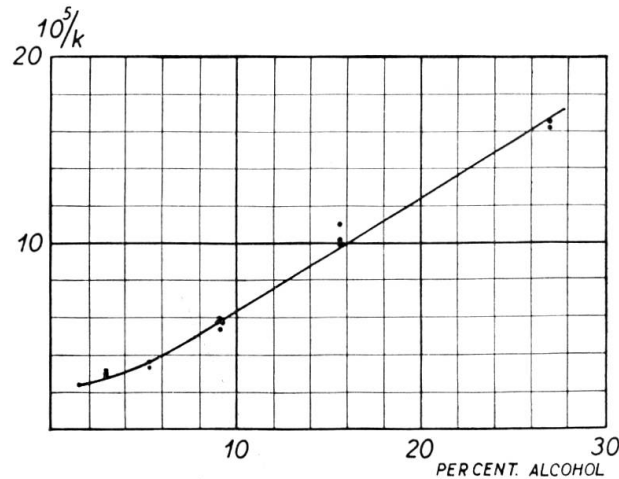quenching circuits keeping the counter inoperative for a long time,

Fig. 2.

Reciprocal plot of electron mobility k versus alcohol content. Data reduced to a
total pressure of 100 mm Hg.

sometimes as long as 0.01 seconds. MULLER has shown that parallel-
plate counter characteristics can be much improved by introducing
a liquid cathode. Counters with an alcohol cathode operate satis-
factorily with a 100-megohm quenching resistor (Fig. 3). But even
so, GEIGER-MÜLLER counters are much more stable and reliable and
will be preferred when they can be at all used.
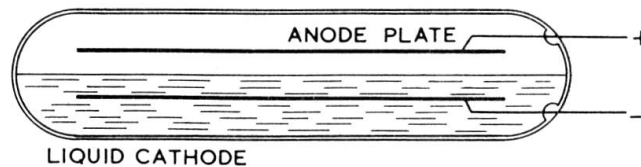
Fig. 3.

Parallel-plate liquid-cathode type of counter developed by F. A. Muller. Spacing
between anode and alcohol cathode 8 mm, argon pressure 100 mm, operating vol-
tage 3500 volts.

Propagation of the Discharge along the Counter Anode.

In the GEIGER region of operating, the additional gas amplification
offered by the spreading of the discharge along the counter wire is
also used, but in most high-speed coincidence work, the pulse is
shortened and normalized in such a way that actually only a very

small part of the extension of the discharge is used. In such applications, there ultimately seems to be little gained and much lost by operating the counter above the GEIGER threshold, thus introducing the ill effects of the deadtime.

Experimental and theoretical work by VAN GEMERT, MULLER, and the author[4]), by ALDER, BALDINGER, HUBER and METZGER[5-8]), by LIEBSON[9]) and recently by WILKINSON[10]) has yielded much material for an adequate description of the mechanism of the discharge, although here again the picture is not quite consistent. The speeds
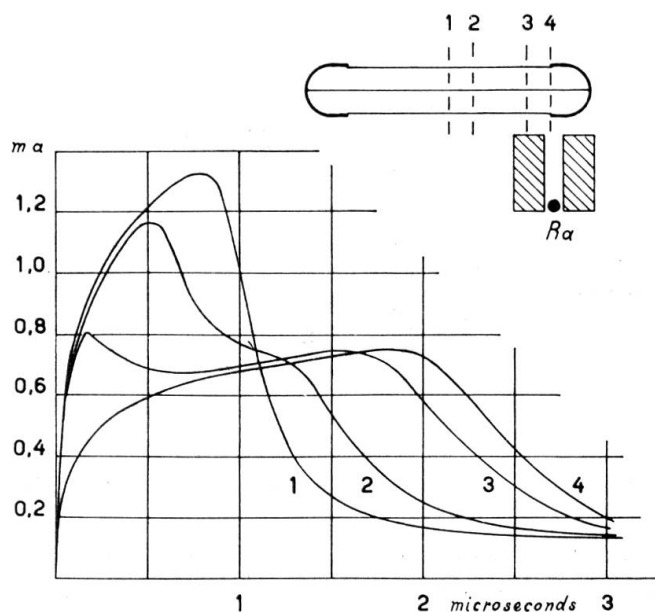
Fig. 4.

Family of current characteristics observed in counter irradiated as indicated in sketch. Counter data: length 200 mm, wire diameter 0.1 mm, cathode diameter 70 mm; counter gas: 45 mm Hg of argon, 45 mm of neon, 10 mm of ethyl-alcohol vapour; operating voltage 1500 volts, overvoltage 215 volts.

of propagation observed average around 10 cm per microsecond, and the rate of current increase is of the order of a few mA per microsecond.

Fig. 4 is the first figure published by VAN GEMERT c. s. showing the dependence of the shape of the counter current pulse on the point of irradiation. It is seen how the propagation in both directions causes the pulse 1 initiated at the centre to have double the rate of increase and half the duration of pulse 4 initiated at the end.

Much more accurate measurements were taken a few years later by ALDER, BALDINGER, HUBER and METZGER[5-8]).

A rise time of 8 mA per μsec was found for a pulse started away from the end of a counter described as follows:

cathode radius $r_c = 9$ mm, wire radius $r_a = 0.075$ mm, alcohol pressure 16 mm of Hg, argon pressure 64 mm of Hg, voltage 1150 volts.

The slowness of propagation along the wire, though usually a nuisance, can sometimes be utilized for determining the point of incidence of the radiation. MULLER's focussing device for WILSON cloud chambers shown in Fig. 5 is based on this principle. Rays
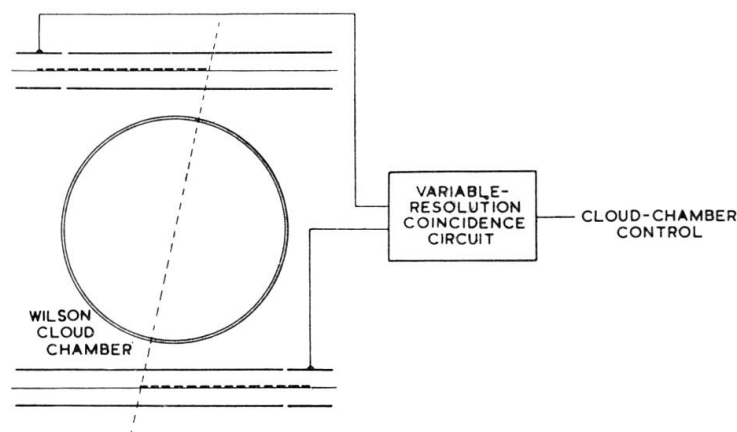

Fig. 5.

F. A. MULLER's system of cloud-chamber control focussing. Width of useful beam can be adjusted by means of the coincidence-circuit resolving time.

passing not too far from the centre of the cloud chamber will be observed only, provided the diameters of the counters are small, so that the extra delays due to the electron transit time are sufficiently small also, and provided the velocities of propagation in the counters are equal. At equal operating voltages, this calls for accurately equal gas mixtures. It is possible but not necessary to let the counter gas volumes communicate so as to keep the mixtures identical during the full useful life of the counters.

The deadtime.

Although most of the counters in current use are of the self-quenching type, self-quenching characteristics are sometimes dispensed with, and non-quenching counters used instead. In these counters, a certain time is lost during which the discharge burns before it is quenched by some external means. But also selfquenching counters involve a time loss after each discharge, the deadtime, during which the counter is inoperative.

Deionization phenomena.

After the fundamental work of C. G. and D. D. Montgomery[11] it was realized that many phenomena in a Geiger counter could be quantitatively accounted for by simple calculations on the motion of the ion sheath in the counter subsequent to the active period of the discharge. In 1942, Stever in the U. S.[12] and van Gemert, Muller and the author in Holland[13] published very similar theoretical and experimental work on the dead time. In a recent paper,
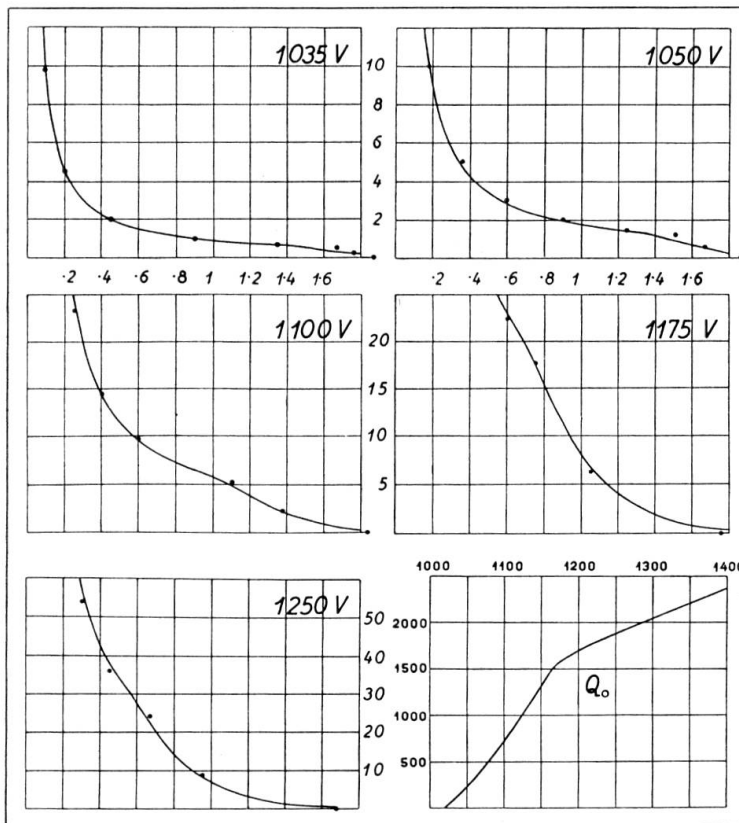

Fig. 6.

Currents observed in a counter with a cathode diameter of 38 mm and a wire diameter of 0.1 mm, filled with 94 mm Hg of argon and 12 mm Hg of alcohol vapour. Horizontal time scales: milliseconds; vertical time scales: 10^{-9} amp per cm counter length. Curves measured, dots calculated from theory on the basis of a uniform ion mobility $k = 5.6$ cm/sec per volt/cm. (Ordinates in the charge characteristic: equivalent calibrating pulses on the counter cathodes, volts.)

Muller and the author [14-15] pointed out how very accurate the agreement between theory and experiment is if a number of corrections are introduced and if precise measurements are taken of both the charge Q developed per unit length of counter wire and the mobility k of the ions in the ion sheath.

Fig. 6 shows a plot of pulse size versus counter voltage, and five experimental curves of deionization currents in a counter of 38 mm cathode diameter and 0.1 mm wire diameter, filled with 12 mm Hg. of ethyl-alcohol and 94 mm of argon. Dots are added indicating current values calculated from the charges measured on the basis of a mobility $k = 5.6$ cm/sec per volt/cm. It will be seen that the agreement is good enough to allow of an accurate determination of k. For further details the reader is referred to the original paper.
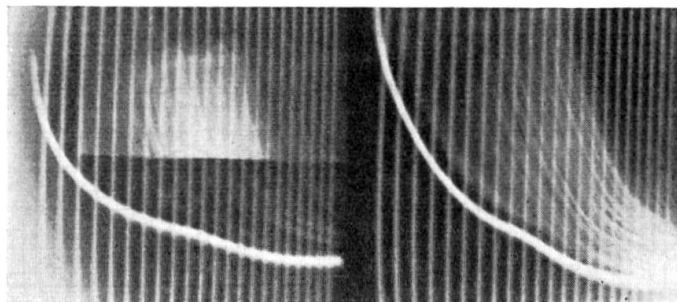

Fig. 7.
After-discharges observed in a counter operating at a high overvoltage. These after-discharges occur within a sharply defined interval of time not coinciding with the arrival of the alcohol ions on the cathode cylinder.

As alcohol ions fall onto the cathode from the break until the termination of the current, it can be seen from an oscillogram of a counter showing afterdischarges (Fig. 7) that these are caused by ions faster than alcohol ions, possibly by argon or decomposition products.

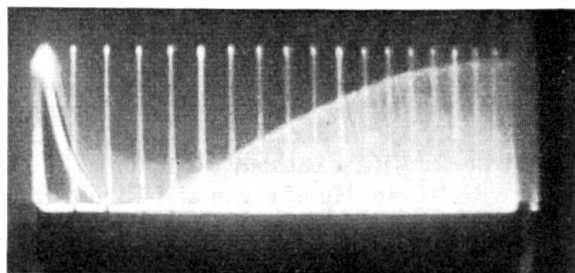Once k and Q are known, the recovery characteristic can be cal-

Fig. 8.
Recovery characteristic of the counter described in the caption to Fig. 6, operating at 1125 volts. Time scale: 0.1 millisecond divisions.

culated, that is the way the field strength at the counter wire is restored after the formation and subsequent migration of an ion sheath. Fig. 8 shows the well-known way in which this recovery can

be visualized on a C.-R. oscilloscope with a time base triggered by the pulses themselves. Translating pulse size into effective voltage V_{eff}, i. e. the voltage to be applied to a deionized counter to get the same pulse size, the recovery characteristics of Fig. 9 are obtained. The dots added are calculated for a space-charge sheath with the mobility k and the charge Q determined before, moving from wire to cathode while a constant potential difference V_s is being applied to the electrodes. Here again, the agreement is quite satisfactory. When V_{eff} passes the starting voltage V_s, the deadtime during which the counter is inoperative is completed. The time for any effective voltage to be reached can be shown to be

$$t = r_c\, r_a \ln \frac{r_c}{r_a}\, \frac{e^{-V/Q}}{2\,k\,Q}\, \overline{Ei} \left(\frac{V_{eff}}{Q} + \ln \frac{r_c}{r_a} \right),$$

where

$$\overline{Ei}(x) = \int_0^x \frac{e^y\, dy}{y}\, .$$

The deadtime τ_0 can be found by substituting $V_{eff} = V_s$. In Fig. 10, the theoretical curve is compared with experiment (dots and circles).
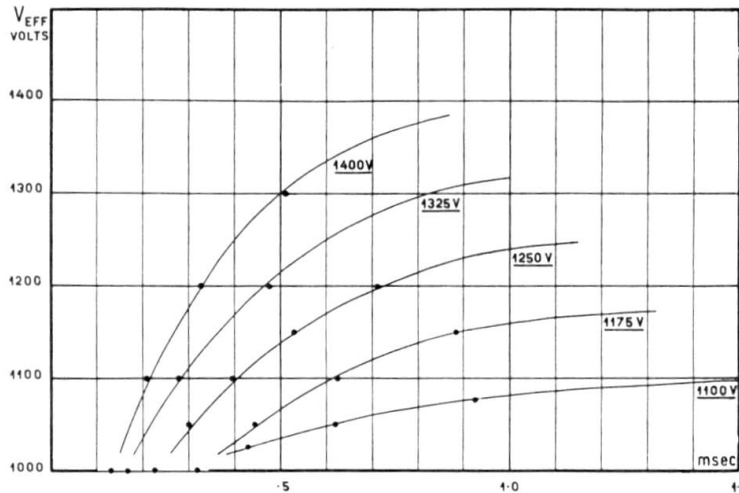
Fig. 9.

Recovery characteristics of the counter described in the caption to fig. 6. Dots are calculated from theory, using the same value for the mobility k.

Corrections for the deadtime.

When n discharges per second are actually produced by the counter, it will be inoperative for the fraction of time $n\tau_0$ so that of the incident counting rate n_0 only the rate $n = (1 - n\,\tau_0)\,n_0$ is actually observed, and the counting loss is

$$\frac{n - n_0}{n_0} = \frac{\tau_0}{\tau_0 + 1/n_0}\, . \tag{1}$$

This formula will only apply if after all pulses the dead time is τ_0. When, however, pulses occur shortly after a preceding pulse, they are not only smaller than normal according to a recovery characteristic, but also give rise to a smaller than normal deadtime, so that there is a recovery as to deadtime as well. When only the probability for two ion sheaths to be present in a counter has to be taken into account, and the probability of three ion sheaths is negligible, this effect can be accounted for by assuming that for a time $(\psi-1)\,\tau_0$ after the deadtime has elapsed, new pulses occur but do not produce a new dead period. This factor ψ can be found by calculating the deadtime with two ion sheaths present in the counter, and is of the order of 2. With this correction

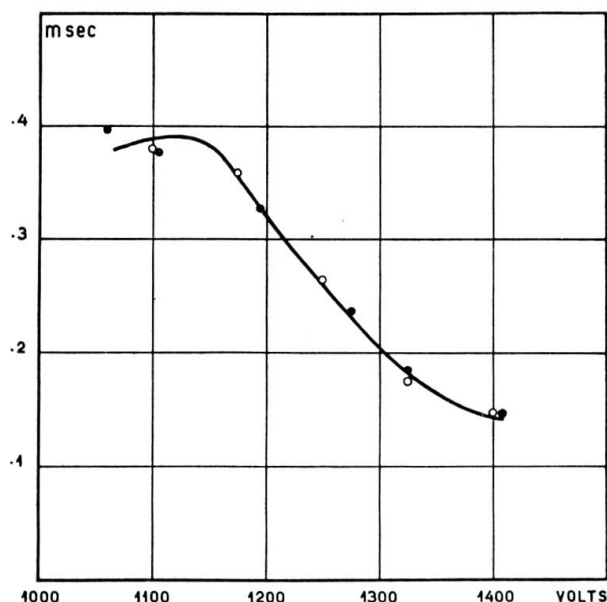$$\frac{n-n_0}{n_0} = \frac{\tau_0}{\psi\,\tau_0 + 1/n_0}\,. \tag{2}$$

Fig. 10.

Dead times measured (dots and circles) and calculated (curve). Counter data and mobility as in Figg. 6 and 9.

For apparent reasons, this formula gives to low a value for the counting loss at very high counting rates, when reduced pulses are normal rather than exceptional.

From the experimental work of MUELHAUSE and FRIEDMAN[16]) and of BALDINGER and HUBER[17]), it is known that with this type of operation, the counting loss becomes nearly constant independent of the counting rate. With a few suitable approximations, this other extreme of a great many ion sheaths present in the counter at the same time becomes very simple, as will be shown in the next section[21]).

Operation at very high counting rates.

The rapid succession of ion sheaths can be approximated by a continuous current I flowing in unit length of counter. When the average effective voltage is V_1, the average field strength at the wire is $2\,CV_1/r_a$, and at any point at radius r reached by the ions after a time t

$$F(r) = \frac{2}{r}\,2\,(CV_1 + It) = \frac{1}{k}\,\frac{dr}{dt}.$$

From this, the motion of the ions is found to be

$$r^2 - r_a^2 = 2\,k\,(2\,CV_1\,t + It^2)$$

and the field strength

$$F(r) = \frac{2}{r}\,(C^2\,V_1^2 + (r^2 - r_a^2)\,I/2\,k)^{\frac{1}{2}}.$$

Putting

$$V = \int\limits_{r_a}^{r_c} F\,dr$$

we have

$$V = 2\,(C^2\,V_1^2 + r_c^2\,I/2\,k)^{\frac{1}{2}} - 2\,CV_1 + V_1$$

$$- 2\,CV_1 \ln\left\{1 + \frac{(C^2 V_1^2 + r_c^2\,I/2\,k)^{\frac{1}{2}} - CV_1}{2\,CV_1}\right\}.$$

For overvoltages not exceeding 200 volts, we may use the approximation $\ln(1+x) = 2\,x/(x+2)$, so that we finally obtain the formula

$$\frac{V - V_1}{2\,CV_1} = \frac{r_c^2\,I/2\,k\,C^2\,V_1^2}{3 + (1 + r_c^2\,I/2\,k\,C^2\,V_1^2)^{\frac{1}{2}}}, \tag{3}$$

indicating the difference between voltage V and average effective voltage V_1 at which a current I will flow.

The recovery characteristics at very high counting rates.

The recovery characteristic must be known so that the average effective voltage V_1 can be calculated as well as the mean time τ elapsing between two discharges.

Now space-charge sheaths not too near to the wire can be averaged on the basis of a time average to a very good approximation as far as their induction on the wire is concerned.

Taking for instance the induction $i = l/t$, for $1 < t < 2$, caused by a space charge moving between one and two units of time after

it has left the wire, this charge can also be represented by a conti-
nuous succession of space charges leaving from $1 - \Delta$ earlier to
Δ later:

$$i' = \int_{\Delta-1}^{\Delta} \frac{1}{t+\tau} \, d\tau.$$

Putting

$$\int_1^2 i \, dt = \int_1^2 i' \, dt,$$

we find $\Delta = 0.56$, and the following set of values

$t =$	1	1.2	1.5	2
$i =$	1	0.833	0.667	0.500
$i' =$	1.027	0.839	0.665	0.495

When an ion sheath leaves the wire, it is preceded by a number of
ion sheaths of different charges according to a statistical distribu-
tion, and showing different time intervals. As we shall see presently,
these quantities are proportional within wide limits, and can be
represented by the same average current I.

This approximation does however not hold for the space-charge
sheath nearest to the wire, so that we shall treat that sheath sepa-
rately. We shall suppose this sheath to be preceded by a succession
of space charges that will be represented by a continuous ion current
I interrupted at the anode a time t_0 before.

Neglecting the small variation of effective voltage about the ave-
rage value V_1, we have for the current induced by the sheath treated
separately

$$i_1 = CQ/(t + r_a^2/4 \, k \, CV_1),$$

and for the current induced by the continuous current:

$$i_2 = IC \ln (r_c^2/4 \, k \, CV_1 \, (t + t_0)).$$

With $Q = I\tau$, the counter will after a time τ be able to produce
another pulse of charge Q, or

$$\int_0^\tau (i_1 + i_2) \, dt = Q.$$

This integration yields

$$t_0 = 0.5425 \, \tau.$$

Putting ΔV_{eff} for the difference of the instantaneous effective vol-

tage and the effective voltage V_{eff} at the time of discharge, we have

$$\int_0^t (i_1 + i_2)\, dt - Q = \Delta V_{\mathrm{eff}}/C$$

so that we obtain on integrating

$$\frac{\Delta V_{\mathrm{eff}}}{Q} = \frac{t}{\tau} + \frac{t}{\tau}\ln\frac{r_c^2}{4\,k\,C V_1(t+t_0)} - \frac{t_0}{\tau}\ln\frac{t+t_0}{t_0} - \ln\frac{r_c^2}{4\,k\,C_1 V\,t + r_a^2}\,. \qquad (4)$$

For $t = 0$, $\Delta V_{\mathrm{eff}}/Q = -1/C$. r_a can be neglected for $t/\tau > 0.1$, and the counter recovery can be described in terms of one variable t/τ and of one parameter $r_c^2/4\,k\,CV_1\,\tau = \vartheta^+/\tau$, where ϑ^+ is the ion transit time at the calculated voltage V_1. For the counter mentioned before, recovery characteristics are collected in Fig. 11.
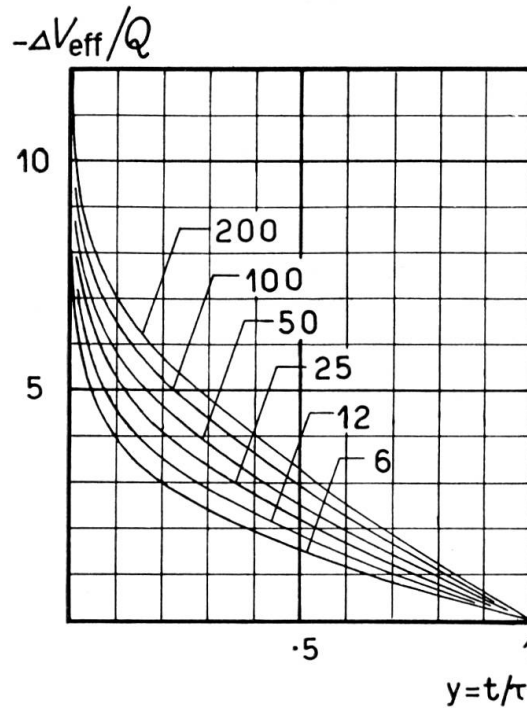

Fig. 11.

Family of calculated recovery characteristics indicating values of $-\Delta V_{\mathrm{eff}}/C$ as a function of t/τ. Values of ϑ^+/τ are indicated on curves. Counter data as for Fig. 6.

For one value of Q, the effective voltage V_{eff} is found from the experimental pulse-size characteristic. The counter overshoots by a factor of $Q/C\,(V_{\mathrm{eff}} - V_s)$, and will not be able to produce another pulse until the initial drop in effective voltage is reduced by a reciprocal factor. The initial drop in $-\Delta V_{\mathrm{eff}}/Q$ being $1/C$, this means that the ordinate in Fig. 11 must have dropped to $(V_{\mathrm{eff}} - V_s)/Q$.

Fig. 12 shows the dependence of $(V_{\text{eff}} - V_s)/Q$ on Q/C as computed from the pulse-size characteristic included in Fig. 6. Thus, assuming values for Q and ϑ^+/τ, Fig. 11 gives the fraction of τ after which the counter is operative again, which is apparently the fractional counting loss f. Also, from the surface under the recovery characteristic, the mean effective voltage V_1 is found. After this, the
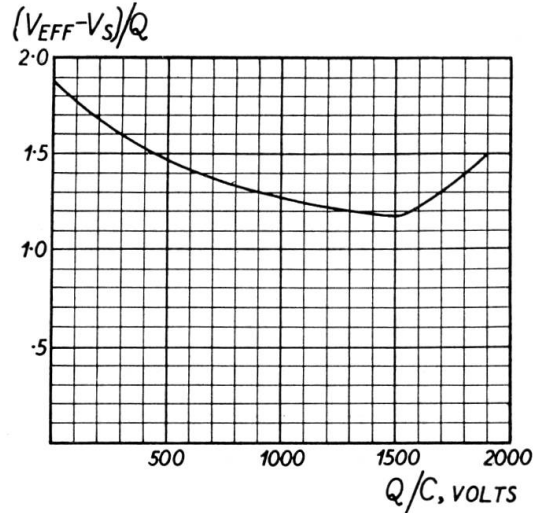

Fig. 12.

Pulse size versus voltage characteristic of fig. 6 rearranged for application of the present theory. For counter data see caption to fig. 6.

expression (3) found for $(V - V_1)/2\,CV_1$ can be used to find the voltage V across the counter, as

$$\frac{r^2\,I}{2\,k\,C^2 V_1{}^2} = 2\left(\frac{\vartheta^+}{\tau}\right)\cdot\frac{Q}{CV_1}\,.$$

Finally, the corrected counting rate is found to be

$$n_0 = \frac{4\,k\,CV_1\cdot(\vartheta^+/\tau)}{r_c^2\cdot(1-f)}\,.$$

Results are collected in Fig. 13, and Fig. 14 shows values of $R = (V - V_s)/I$ for four overvoltages and starting voltage. The Nawijn limit $R = \vartheta^+$ for starting voltage and infinite counting rate is also indicated.

Further corrections.

It is seen from Fig. 11 that the recovery after the deadtime is approximately linear. Within wide limits, the current is constant at constant overvoltage independent of counting rate (Fig. 14) as is the counting loss, so that the slope of the recovery characteristic is

constant and equal to $I/(1-f)$. In the preceding section, the loss was calculated after a pulse preceded by an equal pulse started a time τ before, or a continuous current interrupted a time of about $\frac{1}{2}\tau$ before, and it was shown that these two cases could be interchanged. Therefore, our approximation is extremely good at counting losses of about $\frac{1}{2}$. At higher counting losses, large pulses are preceded
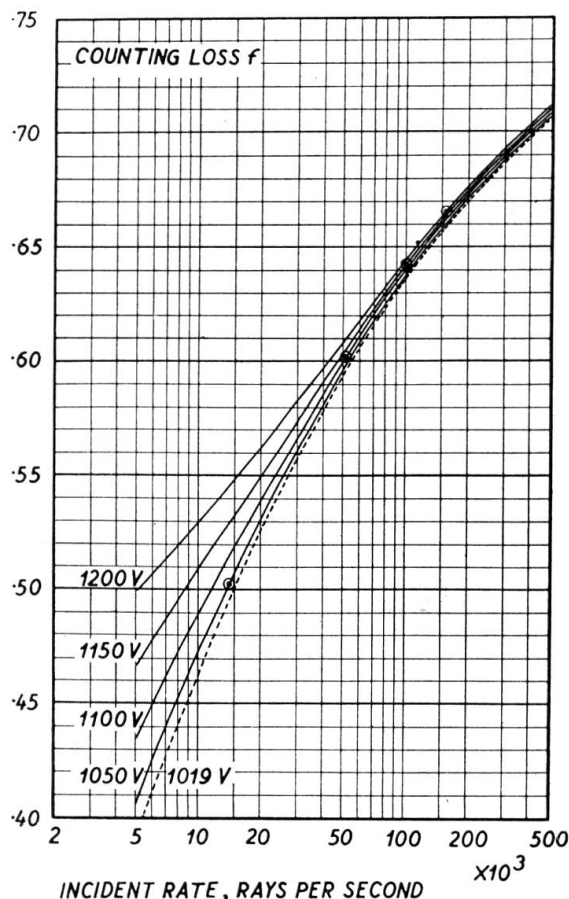

Fig. 13.
Theoretic values for the counting loss at the voltages indicated on left curves. Counter data as described in the caption to Fig. 6. Circles indicate operating conditions giving rise to pulses occurring at a low counting rate at 5 volts overvoltage. Further data are shown in Fig. 15.

more closely by smaller pulses and more remotely by larger ones, so that the average calculation given becomes less representative of the entire range.

The counting rate $n = n_0(1-f)$ is further diminished by two effects.

Firstly, the average effective overvoltage at which the counter discharges becomes very low. Fig. 15 gives the counter voltage necessary at various counting rates so that the average effective over-
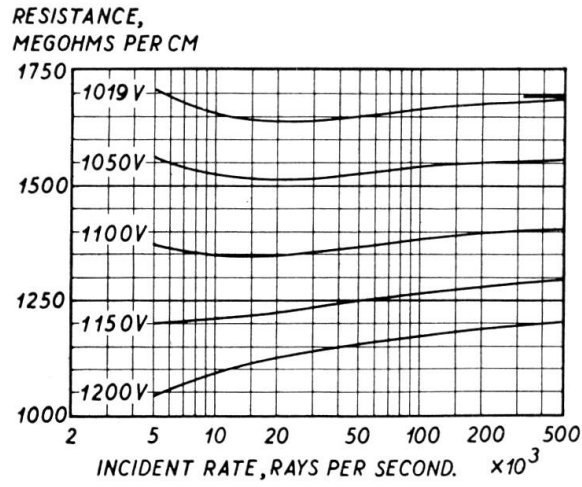
RESISTANCE,
MEGOHMS PER CM

Fig. 14.

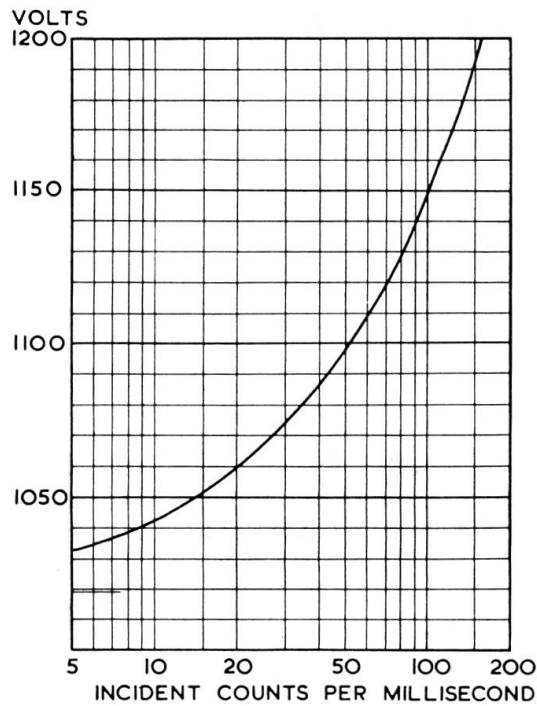Resistance in megohms. cm of the same counter.

Fig. 15.

Increase of operating voltage necessary for keeping the avarage pulse height equivalent to an overvoltage of 5 volts and low counting rate. Data for other equivalent overvoltages can be derived from Figg. 13 and 14.
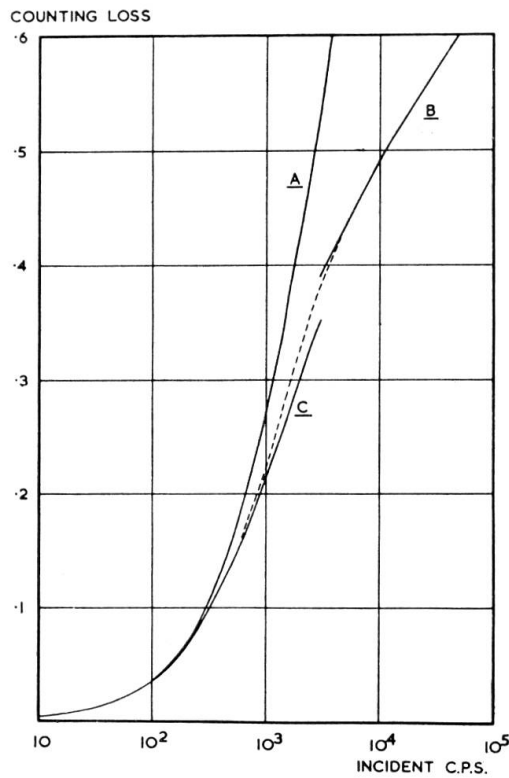
Fig. 16.

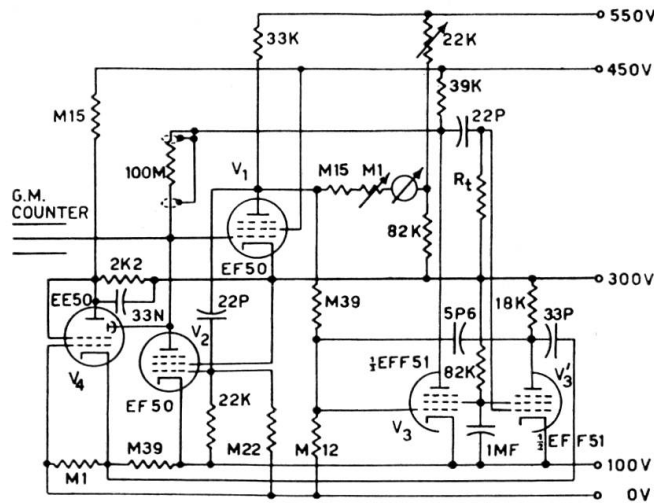Comparison of various correction formulae, as explained in text.

Fig. 17.

Input circuit for dead-time correction indication. The milliameter indicates the fraction of time during which the counter is sensitive to the incident radiation. Satisfactory operation is obtained with any type of counter, either selfquenching or non-selfquenching.

voltage at the time of discharge is 5 volts. Other values may be
derived from Figg. 13 and 14. Consequently, part of the counts will
be lost because of poor counter efficiency. Assuming that the radia-
tion under observation produces minimum pulses Q_0, below which
the efficiency is zero, and above which it becomes unity, the
average pulse size will no longer be $I/n_0 (1 - f)$, but now become
$Q_0 + I/n_0 (1 - f)$, so that the counting rate will be

$$n = \frac{n_0}{n_0 \, Q_0/I + 1/(1-f)} \, .$$

Secondly, when the recording circuit records only pulses $> Q'$. the
fraction

$$\exp \left(\frac{(1-f) \, n_0}{I} (Q_0 - Q') \right)$$

will be recorded only.

Comparison of correction formulae.

In Fig. 16 the various corrections for deadtime losses at 1100 volts
are collected for comparison. Curve A is based on Equ.(1) and gives
far to large corrections at intermediate and high counting rates.
Curve C is Equ. (2) for $\psi = 2$, and is added as a possible approx-
imation for intermediate counting rates. Curve B has been taken
from Fig. 13. For practical purposes, Equ. (2) with $\psi = 1.77$ fits
curve A for the lowest rates, and curve B up to 12,000 incident rays
per second, and will not be much in error for the intermediate coun-
ting rates. It is indicated by the dashed line.

Circuit-controlled insensitive time.

Competing with this way of dealing with high counting rates,
three other methods operating at constant counter efficiency and
pulse size have been introduced, reducing the deadtime by voltage
reversal (DuToit[18]), Hodson[19]), artificially lengthening the dead-
time to an accurately known value determined by a number of
circuit constants (Cooke-Yarborough, Florida and Davey[20])),
or determining the fraction of time during which the counter is
made inoperative by the circuit and thus automatically correcting
for deadtime losses (Muller and the author[14)21])).

The latter system is shown in Fig. 17. The correction is read from
a miliammeter, and should be averaged during the complete run.
This complication is avoided in the modified system of Fig. 18,

where the total sensitive time during the run is measured by counting at the same time coincidences between circuit sensitivity and pulses from a standard pulse generator. This system can also be applied to coincidence counting. In that case, the sensitive period must be determined by counting coincidences of oscillator pulses and sensitive periods of all counting channels.
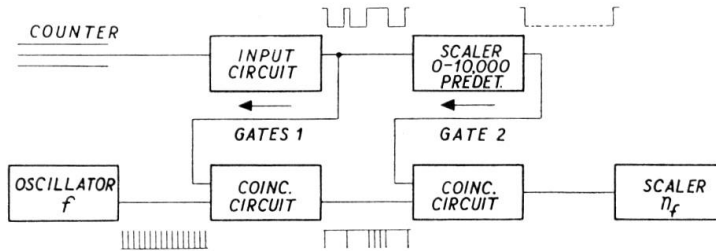

Fig. 18.

Counting system using the input system of Fig. 17, and two scalers counting the counter pulses and the oscillator pulses occurring in the same time intervals, respectively. The counting rate is found by comparing the scaler readings.

Bibliography.

[1]) C. W. Sherwin, Rev. Sci. Inst. **19**, 111 (1948).

[2]) H. den Hartog, F. A. Muller and N. F. Verster, Physica **13**, 251 (1947).

[3]) H. den Hartog, F. A. Muller and C. S. W. van Rooden, Physica **15**, 581 (1949).

[4]) A.G.M. van Gemert, H. den Hartog and F. A. Muller, Physica **9**, 556 (1942).

[5]) P. Huber and F. Alder, Helv. Phys. Acta **18**, 232 (1945).

[6]) P. Huber, F. Alder and E. Baldinger, Helv. Phys. Acta **19**, 204 (1946).

[7]) P. Huber, F. Alder, E. Baldinger and F. Metzger, Helv. Phys. Acta **19**, 207 (1946).

[8]) F. Alder, E. Baldinger, P. Huber and F. Metzger, Helv. Phys. Acta **20**, 73 (1947).

[9]) S. H. Liebson, Phys. Rev. **72**, 602 (1947).

[10]) D. H. Wilkinson, Phys. Rev. **74**, 1417 (1948).

[11]) C. G. and D. D. Montgomery, Phys. Rev. **57**, 1030 (1940).

[12]) H. G. Stever, Phys. Rev. **61**, 38 (1942).

[13]) A.G.M. van Gemert, H. den Hartog and F. A. Muller, Physica **9**, 658 (1942).

[14]) H. den Hartog, Counters with Argon and Alcohol, Thesis, Amsterdam 1948 (in Dutch).

[15]) H. den Hartog and F. A. Muller, Physica **15**, 789 (1949).

[16]) C. O. Muelhause and H. Friedman, Rev. Sci. Instr. **17**, 506 (1946).

[17]) E. Baldinger and P. Huber, Helv. Phys. Acta **20**, 470 (1947).

[18]) S. J. du Toit, Rev. Sci. Instr. **18**, 31 (1947).

[19]) A. L. Hodson, J. Sci. Instr. **25**, 11 (1948).

[20]) E. H. Cooke-Yarborough, C. D. Florida and C. N. Davey, J. Sci. Instr. **26**, 124 (1949).

[21]) H. den Hartog and F. A. Muller, Physica **15**, November 1950.